

A Spatial AR System for Wide-area Axis-aligned Metric Augmentation of Planar Scenes

Michael Hornáček*, Hans Küffner-McCauley, Majesa Trimmel,
Patrick Rupprecht, Sebastian Schlund

*Human Centered Cyber Physical Production and Assembly Systems, Institute for
Management Sciences, TU Wien, Vienna, Austria*

Abstract

Augmented reality (AR) promises to enable use cases in industrial settings that include the embedding of assembly instructions directly into the scene, potentially reducing or altogether obviating the need for workers to refer to instructions in paper form or on a screen. *Spatial* AR, in turn, is a form of AR whereby the augmentation of the scene is carried out using a projector, with the advantage of rendering the augmentation visible to all onlookers simultaneously without calling for each to wear some form of head-mounted display. In carrying out spatial AR, however, care must be taken to appropriately warp an image to be projected in a manner that it, when projected, appear free of distortions to the viewer. For planar scene geometry (such as a floor, wall, or table), a cumbersome manual process called keystone correction—involving warping an image by perturbing its corners until the desired effect is produced when projected to the scene—can be used to carry out an appropriate corrective image warp.

We propose a spatial AR system for wide-area metric augmentation of planar scene surfaces that produces the effect of keystone correction analytically as a function of the relative geometry of the projector and scene plane, using a projector equipped with a steerable mirror and a camera facing the scene

*Corresponding author

Email address: michael.hornacek@tuwien.ac.at (Michael Hornáček)

plane. Our system renders the placement of augmentations in the scene more intuitive than manual keystone correction in two ways. First, (i) placement of the desired augmentations is carried out in accordance with the axes of an image of the scene acquired by the camera, thereby making setting those axes as simple as appropriately rotating the camera. Second, (ii) the desired dimensions of the projected augmentations are specified in metric terms, thereby allowing for consistent scaling across all target locations.

Keywords: Spatial augmented reality (SAR), computer vision, steerable mirror projector, projector-camera calibration, Industry 4.0

1. Introduction

Augmented reality (AR) [1, 2] promises to enable use cases in industrial settings that include the embedding of assembly instructions directly into the scene [3, 4, 5, 6, 7, 8], potentially reducing or altogether doing away with the need for workers to refer to instructions in paper form or on a screen. Typically, AR works by embedding the augmentation in an image of the scene acquired from the viewpoint of a single individual, with the resulting augmented image in turn displayed typically using some form of head-mounted display. Reliance on head-mounted displays, however, has two adverse consequences: (i) a head-mounted display must be worn by each individual wishing to partake in the augmentation, and (ii) such a head-mounted display—in some cases taking the form of a helmet in order to house multiple sensors in support of accurately tracking the viewpoint of the viewer relative to the scene—can be obtrusive. In turn, a form of augmented reality referred to as *spatial* AR[9] is carried out not by embedding the augmentation in an image of the scene as with a head-mounted display, but by projection to the scene itself, thus eliminating both aforementioned problems. Yet considering a planar surface to be augmented (e.g., a floor, wall, or table), unless the projector faces the surface frontally, the bounds of a projected rectangular image will not appear rectangular, but will instead be subject to projective distortions. Such distortions can be corrected for

by carrying out a cumbersome manual process referred to as keystone correction to appropriately warp the image to be projected, often using software bundled with the projector.

Our contribution is to propose a wide-area spatial AR system for planar
25 scenes that produces the effect of keystone correction analytically, free of any manual interaction. Most importantly, we do this in a manner placing the axes of the augmentation in accordance with the axes of a camera placed to face directly towards the scene plane (a camera we shall in what follows refer to as ‘downwards facing’, for brevity). This facilitates placement of augmentations,
30 since establishing the principal axes of the augmentation thus reduces to placing the downwards-facing camera in a manner such that the X - and Y -axes of the image align with the intended X - and Y -axes of the augmentation. We achieve this by warping the image to be projected using a plane-induced homography computed to produce the effect of projecting the image not from the actual
35 projector viewpoint, but in accordance with the viewpoint of a *virtual* projector. We place this virtual projector to (i) face directly downwards to the target location in the scene plane and (ii) rotate its axes in accordance with those of the camera. Moreover, our system enables specifying the dimensions of augmentations in metric terms, which we achieve by placing the virtual projector
40 at the appropriate height above the scene plane. Finally, our system set up to handle a projector equipped with a steerable mirror (without need for explicitly modeling the action of the steerable mirror on the projector), thereby enabling wide-area applications exceeding the immediate field of view of the projector without needing to rely on multiple projectors.

45 1.1. Related Work

An early spatial AR system explicitly using a projector mounted with a steerable mirror is the IBM Everywhere Displays prototype of Pinharez [10]. For the purposes of the prototype, a projector mounted with a steerable mirror was set up with a camera to demonstrate a variety of use cases, including col-
50 laborative assembly encompassing the projection of assembly instructions and

an interactive projected user interface [11, 12]. The authors, however, carry out keystone correction manually, by interactively adjusting for the position and orientation of a virtual scene plane and a scaling factor and computing a 2D homography accordingly.

55 More generally, keystone correction for planar scenes can be said to reduce to computing a 2D homography [13], an invertible transformation that preserves colinearity and is thus fittingly alternatively referred to as a ‘colineation’; this is the case whether computing the homography relies on manual interaction as in the case of Pinharez, or is obtained free of manual interaction as in ours.

60 The intuition for why it is that a transformation that preserves colinearity—i.e., maps lines to lines—can serve to model an appropriate corrective image warp can be drawn from considering a planar chessboard pattern: looking at an image of a chessboard acquired from an oblique angle, one observes that lines parallel in the chessboard appear to meet in respective vanishing points; looking

65 at an image of the same chessboard acquired frontally with respect to the plane of the chessboard, lines parallel in the chessboard appear parallel in the image (i.e., they are said to meet ‘at infinity’). To warp the former image (where lines parallel in the scene meet in respective vanishing points) such that the lines of the chessboard appear as in the latter image (where lines parallel in the scene

70 meet at infinity) calls for a transformation that maps lines to lines.

One way to compute a homography is by identifying at least four correspondences between pixel positions in two images of a planar surface [13]. The keystone correction approach of Sukthankar *et al.* [14] reduces to using a segmentation approach to identify the four corners of projection screen in an image

75 acquired by a camera, and computing a homography that maps the resulting four corners of the projection screen to the four corners of the projector’s image plane. Additional sensors can be used to inform the computation of a homography; Raskar and Beardsley [15] use a tilt sensor to recover the projector’s gravity vector, which they use to carry out a rotational correction in projecting

80 to a wall. Still another way to compute a homography is as a function of a plane and a pair of pinhole cameras; the effect produced by the homography is one

of projecting an image to the plane from the viewpoint of the one camera, and acquiring the projected image from the viewpoint of the other. Such a homography is said to be ‘induced’ by a plane [13]. We exploit the fact that cameras
85 and projectors alike can be modeled using a pinhole camera model [9], proceed to recover the relative geometry relating the scene plane and projector, and compute a particular form of plane-induced homography to effect the intended corrective image warp, taking into account both desired in-plane orientation and metric scale.

90 2. Approach

Correcting for projective distortions of the sort outlined in Section 1 can be achieved by modeling the manner in which the respective rays through the pixels of the projector’s image plane fan out into the scene (i.e., by ‘calibrating’ the projector) and the geometry of the scene itself (i.e., by recovering the scene
95 plane relative to the projector) within at least the projector’s field of view. This is because the scene point ‘illuminated’ by a pixel in the projector’s image plane can be recovered by intersecting its corresponding ray with the geometry of the scene surface; modeling the geometry that relates projector and scene plane thus enables one to reason about the problem of correcting for distortions in terms
100 of geometry. To model this interaction, we (i) carry out a one-time projector calibration, which in our approach calls for additionally calibrating a camera facing downwards to the scene plane and includes recovery of the scene plane as a convenient side effect. Next, we use the relative camera-projector-scene plane geometry to (ii) compute a plane-induced homography that warps the image to
105 be projected in a manner that it appear undistorted to the viewer, and placed in alignment with the axes of a proxy image of the scene. These two points are treated in Sections 2.1 and 2.2, respectively.

2.1. Recovering Geometry

Calibration of a projector (or camera) in the sense we employ the term here¹ renders one able to project a scene point $\mathbf{X} \in \mathbb{R}^3$ to its corresponding pixel $\mathbf{x} \in \mathbb{R}^2$ in the projector’s (or camera’s) image plane, or to compute the ‘back-projection’ of \mathbf{x} , i.e., the ray from the projector’s (or camera’s) center of projection through \mathbf{x} along which a projecting point \mathbf{X} must lie. Such a calibration can be expressed in terms of (i) a 3×3 calibration matrix \mathbf{K} derived from the projector’s (or camera’s) focal length f and principal point $\mathbf{p}_0 = (x_0, y_0)^\top \in \mathbb{R}^2$ [13], and (ii) the coefficients of a lens distortion model used to correct for radial or tangential distortions caused by the lens system [16, 17]; the calibration matrix \mathbf{K} is then

$$\mathbf{K} = \begin{bmatrix} f & 0 & x_0 \\ 0 & f & y_0 \\ 0 & 0 & 1 \end{bmatrix}, \quad (1)$$

where f and $(p_x, p_y)^\top$ are both expressed in units of pixels. The calibration
110 matrix \mathbf{K} models a so-called pinhole camera; such a model is applicable to an image acquired using a real-world camera assuming the image has been corrected for lens distortion effects, by having applied the appropriate lens distortion model coefficients.

A camera can be calibrated by (i) establishing 2D-3D correspondences between pixels in the camera’s image plane and the corresponding points in the scene, and on (ii) using those correspondences as input to an optimization procedure that relies on bundle adjustment [18] to output maximum likelihood estimates of the calibration matrix, the associated lens distortion model coefficients, and, for each calibration image, the pose (i.e., position and orientation) of the camera relative to the 3D scene points from among the 2D-3D correspondences [13, 19]. Calibration images containing a calibration surface such as a chessboard pattern of known dimensions and scale are acquired

¹We are referring to a geometric calibration; not, e.g., to a color calibration.

from varying viewpoints using the camera, to be used to establish the 2D-3D correspondences $\{\mathbf{x}_{i,j} \leftrightarrow \mathbf{X}_{i,j}\}$, $i \in \{1, \dots, n_{\text{pt}}\}, j \in \{1, \dots, n_{\text{im}}\}$, where n_{pt} gives the number of correspondences obtained from one calibration image of the pattern, n_{im} the number of such images, and $\mathbf{X}_{i,j} = \mathbf{X}_{i,j'}$, for $j, j' \in \{1, \dots, n_{\text{im}}\}$. Bundle adjustment is then used to obtain the maximum likelihood estimates $(\hat{\omega}, \hat{\mathbf{K}}, \{(\hat{\mathbf{R}}_j, \hat{\mathbf{t}}_j)\})$, $j \in \{1, \dots, n_{\text{im}}\}$ of the lens distortion model coefficients ω , calibration matrix \mathbf{K} , and rigid body transformations $(\mathbf{R}_j, \mathbf{t}_j) \in SE(3)$, $j \in \{1, \dots, n_{\text{im}}\}$. These are obtained using bundle adjustment by minimizing the cumulative reprojection error

$$\sum_{i=1}^{n_{\text{pt}}} \sum_{j=1}^{n_{\text{im}}} d_{\hat{\omega}}(\mathbf{x}_{i,j}, \hat{\mathbf{x}}'_{i,j}), \quad (2)$$

where $\hat{\mathbf{R}}_j \mathbf{X}_{i,j} + \hat{\mathbf{t}}_j \in \mathbb{R}^3$ expresses the point $\mathbf{X}_{i,j}$ in the local coordinate frame
115 of the camera corresponding to the j^{th} calibration image and $(\hat{\mathbf{x}}'_{i,j}, 1)^{\top} \sim \hat{\mathbf{K}}(\hat{\mathbf{R}}_j \mathbf{X}_{i,j} + \hat{\mathbf{t}}_j) \in \mathbb{P}^2$ gives the projection $\hat{\mathbf{x}}'_{i,j} \in \mathbb{R}^2$ in pixels of $\mathbf{X}_{i,j}$ to that image. The function $d_{\hat{\omega}}$ is a distance function that computes a distance with respect to two pixel positions that it first corrects for lens distortions, in accordance with the lens distortion model coefficients $\hat{\omega}$ [16, 17]. Inverting the rigid body
120 transformation $(\mathbf{R}_j, \mathbf{t}_j)$ gives the pose $(\hat{\mathbf{R}}_j^{-1}, -\hat{\mathbf{R}}_j^{-1} \hat{\mathbf{t}}_j) \in SE(3)$ of the j^{th} camera relative to the 3D scene points of the calibration pattern, with $-\hat{\mathbf{R}}_j^{-1} \hat{\mathbf{t}}_j \in \mathbb{R}^3$ the corresponding center of projection.

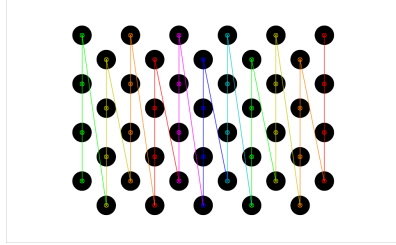
Calibrating a projector [20, 21, 22] can be carried out in precisely the same manner as calibrating a camera insofar as step (ii) is concerned; the major dif-
125 ference in projector calibration relative to the calibrating a camera concerns the manner in which 2D-3D correspondences are identified, i.e., between pixels in the image plane of the projector and the corresponding points in the scene. Since our approach to projector calibration relies on a calibrated camera, what remains of this section is concerned primarily with the recovery of
130 2D-3D correspondences first in support of calibrating cameras, then of projectors. A consequence of the approach we take to identifying the 3D points of the 2D-3D correspondences we use for projector calibration is, for each target

location, recovery of the local scene plane.

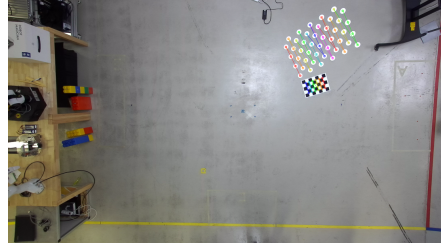
Camera calibration. We recover 2D-3D correspondences in support of calibrating the downwards-facing camera by relying on a planar calibration surface to automatically identify correspondences between the 3D points on the calibration surface and their 2D correspondences in the image plane. The classical calibration surface is a chessboard pattern. The 3D corner points of the chessboard are obtained *a priori* in a coordinate system defined in the plane of the chessboard², requiring knowledge only of the dimensions of the chessboard pattern and of the length of a side of a chessboard square. The corresponding 2D points are obtained, in the same order, using a specialized algorithm [23]. A set of calibration images is acquired, each with the calibration pattern visible in a different part of the image plane, and such that the center and all corners and edges of the image plane are covered, the camera’s autofocus setting be off, and the camera’s zoom factor remain fixed. 2D-3D correspondences are then recovered for each calibration image, and the resulting list is passed on as input to an optimization procedure that relies on bundle adjustment to yield the camera calibration matrix K_{cam} .

Projector calibration. As in camera calibration, we calibrate the projector by relying on 2D-3D correspondences, yet for projector calibration we obtain them by *projecting* a calibration pattern that we detect using the calibrated downwards-facing camera. The pattern we project is one of circles (cf. Figure 1(a)), and we rely on an algorithm to detect the circle center points in the asymmetrical circle pattern in the image plane of the projector [23], giving the 2D positions of our 2D-3D correspondences for calibrating the projector. We project the

²E.g., $(0, 0, 0), (1.5, 0, 0), (3, 0, 0), \dots, (9, 7.5, 0)$ for a chessboard with 7×6 corners (8×7 squares), with each square of length and width of 1.5 unit, respectively. Note that the units of the chessboard’s 3D points give the units in terms of which the camera calibration is carried out, and—owing to how our projector calibration relies on the camera calibration—the units of the projector calibration as well.



(a) Asymmetrical circle pattern image, in image plane of projector (detections overlaid).



(b) Projector calibration image (one for each target location), in image plane of camera (detections overlaid).

Figure 1: Recovering 2D positions in support of projector calibration. (a) 2D positions of the 2D-3D correspondences to be used for calibrating the projector are obtained by detecting—in the image plane of the projector—the circle centers in the asymmetrical circle pattern. It is this pattern that we project to each of the target locations in the scene plane. (b) For each such target location, an image is acquired from the viewpoint of the camera and the circle centers of the projected asymmetrical circle pattern are detected, in the image plane of the camera. A chessboard pattern to be used for recovering the local scene plane is placed near the projected pattern, whose corners are likewise detected. Detected 2D projected asymmetrical circle pattern circle center points and chessboard corners overlain for illustration.

asymmetrical circle pattern to each of the target locations, and use the the calibrated downwards-facing camera to acquire a projector calibration image for each. Given a projector calibration image acquired using camera, we detect
160 the circle centers of the *projected* asymmetrical circle pattern (cf. Figure 1(b)); given the scene plane (the recovery of which we shall return to in the paragraph that follows) and such a 2D circle center \mathbf{x} , we obtain its 3D correspondence by intersecting the back-projection $\mathbf{K}_{\text{cam}}^{-1}(\mathbf{x}^\top, 1)^\top \in \mathbb{P}^2$ of \mathbf{x} with the recovered scene plane (cf. Figure 2). Since the algorithm that yields 2D circle centers does
165 so in a consistent ordering, we thus obtain the 2D-3D correspondences between the projector’s image plane and the scene required for projector calibration, yielding the projector calibration matrix \mathbf{K}_{proj} .

We recover the scene plane via spatial resection by applying a PnP algorithm [24] to the 2D-3D correspondences obtained using a chessboard pattern. Note

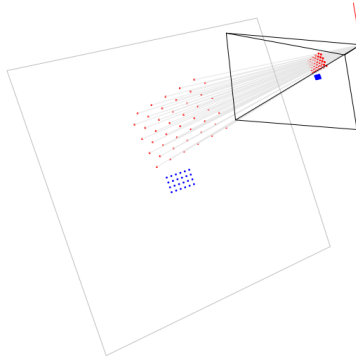


Figure 2: Scene plane (gray) recovered via spatial resection with respect to 2D-3D correspondences obtained using a chessboard pattern (blue); 3D circle center points of the asymmetrical circle pattern—i.e., the 3D positions of the 2D-3D correspondences to be used for calibrating the projector—obtained by intersection with the scene plane of back-projections (likewise gray) of the 2D circle center points of the asymmetrical circle pattern detected in the image plane (red). Note that as in the figures of this section that follow, the rendering in the figure corresponds to the projection calibration image in Figure 1(b), acquired by the downwards-facing camera (frustum of the camera in black, with up vector in red).

170 that this step is separate from camera calibration, yet could well be carried out using the same calibration pattern used in the camera calibration step.³ While a single image of such a chessboard pattern placed on the floor could be sufficient if the floor is even, we account for the possibility of an uneven floor by placing a chessboard pattern in close proximity to the projected asymmetrical
 175 circle pattern in each projector calibration image in order to recover the scene plane locally to each target location (cf. Figure 1(b)). Note that in principle, we could project a chessboard pattern instead of an asymmetrical circle pattern to obtain the 2D-3D correspondences needed for projector calibration; it is, however, because we rely on detecting the corners of a chessboard pattern to
 180 recover the scene plane that we opt instead for a alternative pattern.

The pose of the projector, for each projector calibration image, is provided

³The critical point is that the pattern should ideally be coplanar with the local scene plane, meaning its height above the scene plane should not exceed a few millimeters.

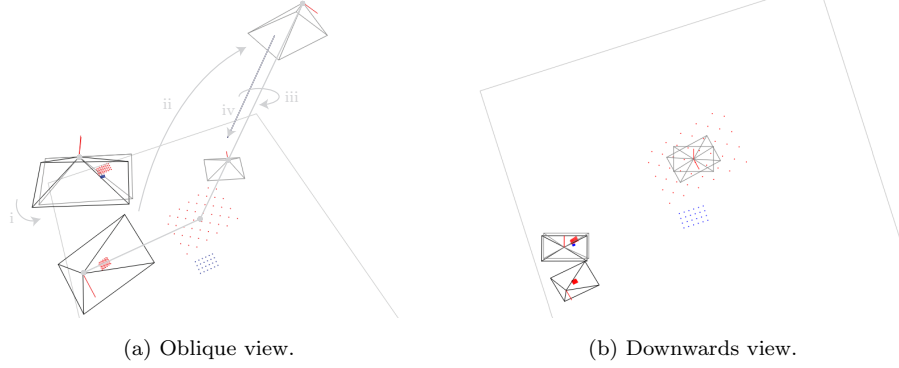


Figure 3: The virtual camera is obtained by (i) rotating the camera (top left, black) about its center of projection such that its optical axis be made parallel with the normal vector of the scene plane. The virtual projector is obtained by (ii) rotating the projector (bottom left, black) about the point of intersection of its optical axis with the scene plane such that the optical axis be made parallel with the scene plane’s normal vector, (iii) rotating the X - and Y -axes to align them with those of the virtual camera, and (iv) translating along the normal direction to achieve the desired metric projected image dimensions.

relative to the 3D points of the pattern—and thus in the coordinate frame of the camera—alongside K_{proj} by the aforementioned optimization procedure. Note that for a fixed projector with steerable mirror, given a projector calibration
185 image, the recovered projector’s pose is the pose the projector would have to have had to project to the given target location *in the absence of the mirror* (i.e., facing directly towards the target location). This is sufficient for our needs in Section 2.2, and it is in this sense that our system is able to handle a projector equipped with a steerable mirror, without need for modeling the steerable mirror
190 explicitly.

2.2. Correcting for Projective Distortion

If the projector is calibrated and its pose relative to the scene plane is known, a ‘virtual’ projector (with the same calibration K and lens distortion model coefficients) can be placed elsewhere relative to the scene plane. If we for a moment

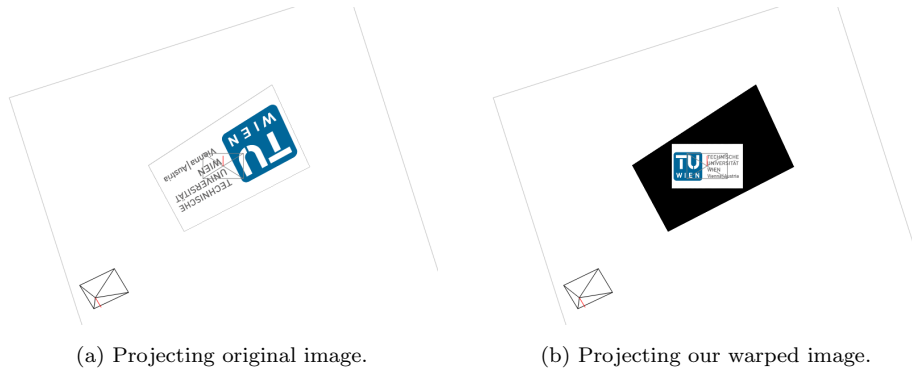


Figure 4: Projection to the scene plane from the recovered projector viewpoint (bottom left, black; virtual projector in center, gray) of the original image and of the warped image. (a) Projecting the original image to the scene plane. (b) After warping the original image according to our plane-induced homography for the given target location, the image is projected in a manner that appears free of projective distortions, aligned with the axes of the virtual camera (via the virtual projector), and to have the desired dimensions in the scene plane, expressed in metric units. Note that unprojected background is shown set to black.

195 imagine that the projector—at its recovered pose—functions as a camera,⁴ then
 (i) projecting an image to the scene plane *from the viewpoint of the virtual pro-*
jector and (ii) acquiring the resulting projected image from the viewpoint of
 the recovered projector gives the desired corrective warp. Projecting an image
 warped in this manner to the scene plane *from the viewpoint of the recovered*
 200 *projector* then has the same effect as projecting the original image to the scene
 plane from the viewpoint of the virtual projector. This warp can be effected
 using a plane-induced homography, computed analytically as a function of the
 scene plane, the projector, and the virtual projector.

⁴Recall that the calibration matrix \mathbf{K} enables computing both (i) the projection of a scene point to the image plane (the function of a camera), or (ii) the back-projection of a pixel in the image plane, giving a ray into the scene (along which a projector illuminates the scene with the given pixel).

Plane-induced homography. Let K_{proj} express the calibration matrix of the recovered projector and $(\mathbf{R}, \mathbf{t}) \in SE(3)$ the rigid body transformation that transforms points from the coordinate frame of the recovered projector to that of the virtual projector, for a given target location. Moreover, let $(\mathbf{n}^\top, -d)^\top$ give the scene plane, expressed in the coordinate frame of the recovered projector, where $\mathbf{n} \in \mathbb{R}^3$ is the scene plane’s normal vector and $d = \mathbf{n}^\top \mathbf{X}$ for any point \mathbf{X} in the plane, so that $(\mathbf{n}^\top, -d)(\mathbf{X}^\top, 1)^\top = 0$. The transformation that warps the image to be projected to the scene plane by the recovered projector such that it appear as if were projected to the scene plane by the virtual projector (cf. Figure 4(b)) is given by the 3×3 matrix

$$\mathbf{H} = K_{\text{proj}} \left(\mathbf{R} - \frac{\mathbf{t}\mathbf{n}^\top}{d} \right) K_{\text{proj}}^{-1}, \quad (3)$$

a form of ‘plane-induced’ 2D homography [13]. For convenience, we enable
 205 optional rotation of the image to be projected *before* applying \mathbf{H} , about the image center; that rotation, parameterized in degrees, is thus in effect carried out—likewise intuitively—with respect to the ground plane.

Virtual projector. The placement of the virtual projector is to determine from which pose the image to be projected is to *appear* to have been projected. We
 210 carry out this placement according to a small handful of steps. First, we (i) rotate the camera about its center of projection to align its optical axis⁵ with the normal vector of the scene plane, giving a virtual camera likewise facing directly⁶ downwards to the scene plane (cf. Figure 3). Next, we (ii) intersect the scene plane with the optical axis (i.e., the ray from the projector’s center
 215 of projection through the center of the image plane) and rotate the projector’s placement about that point of intersection, aligning the optical axis with the

⁵Strictly speaking, the optical axis is the back-projection of the principal point; in our usage, we understand it to refer to the back-projection of the center of the image to be projected.

⁶A physical camera placed to face downwards is almost certain to not face downwards precisely; in contrast, the virtual camera’s optical axis is aligned exactly with the scene plane’s normal vector, rendering it genuinely fronto-parallel with respect to the scene plane.

scene plane’s normal vector and giving an initial virtual projector. Finally, we (iii) align the X - and Y -axes of the initial virtual projector with those of the virtual camera, which gives the virtual projector (cf. again Figure 3). The
220 virtual projector is thus rendered fronto-parallel with the scene plane, enabling projection to the scene plane absent of projective distortions. We additionally (iv) adjust the height above the scene plane of the virtual projector, in order to satisfy desired projected image dimensions provided in metric units.

Owing to the manner in which we place the virtual projector, the virtual
225 projector’s axes and thus the augmentation are aligned with the axes of the downwards-facing camera; the placement of the camera thereby intuitively determines the principal axes according to which augmentations are to be placed. Note further that a consequence of placing the virtual projector by rotating about the point of intersection of the projector’s optical axis with the scene
230 plane is that *the center of the projector’s image plane remains invariant* to the placement of the virtual projector, i.e., a steerable mirror can be aimed with respect to a point projected from the center of the projector’s image plane, further facilitating placement of augmentations.

3. Evaluation

235 We evaluate our approach by using a $960 \text{ pixel} \times 600 \text{ pixel}$ image of the TU Wien logo (cf. Figure 4) to augment 15 locations across the floorspace at the Pilotfabrik⁷ of TU Wien, a collaborative space for research on Industry 4.0 topics situated in Vienna, Austria. We contrast our approach with a baseline
240 approach involving manual keystone correction, by aiming with both approaches to place the same image for each location aligned with the principal axes of the floorspace, absent of projective distortions, and with the same metric dimensions of $50 \text{ cm} \times 31.25 \text{ cm}$ ⁸. All experiments were carried out by the same technician,

⁷<https://www.pilotfabrik.at/>

⁸The dimensions in pixels of the image we project are 960×600 ; we chose for our experiments to set the projected metric length of the horizontal axis of the image to 50 cm, which

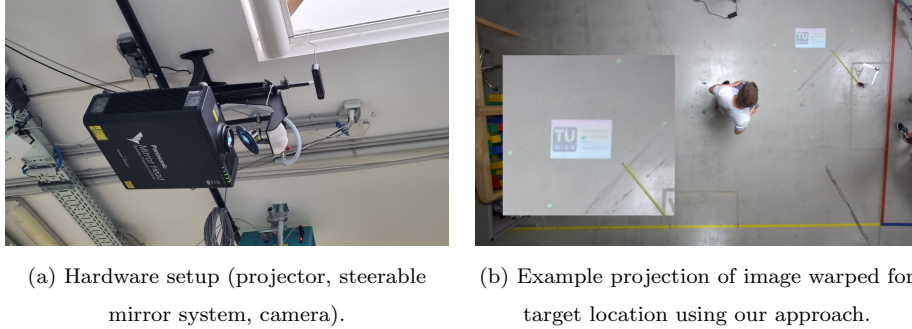


Figure 5: Evaluation scenario. (a) Our hardware setup, comprised of a Panasonic PT-RZ660BE projector, a steerable mirror system manufactured by Dynamic Projection Institute, and a Stereolabs Zed 2 stereo camera, of which we used only the left view. (b) Example augmentation produced by projecting—to one of our 15 target locations—an image warped using our approach, as seen from the downwards-facing camera. Note that the warp places the axes of the augmentation in accordance with the axes of the camera, and that the dimensions of the augmentation are in line with the desired target dimensions (50 cm \times 31.25 cm). Corners of the full projected image extent projected to the floor in light green.

experienced in both approaches.

The hardware setup employed in the evaluation (cf. Figure 5(a)) comprised a
 245 Panasonic PT-RZ660BE projector with a steerable mirror system—used in our
 experiments to point the projection to each of the 15 locations—manufactured
 by Dynamic Projection Institute [7, 8]. The steerable mirror system was bundled
 with the MDC-X software for steering the mirror, loading imagery, and
 optionally carrying out manual keystone correction, such that each position and
 250 (warped) image can be registered as a preset. In addition, we used a downwards-
 facing Zed 2 stereo camera manufactured by Stereolabs, yet relied only on the
 left view. The floorspace used for our experiments measured dimensions of ca.
 6 m \times 4 m; the projector was mounted at approximately the center of this space,
 at a height of ca. 3.5 m. At this height, the pixel size (i.e., length or width of a
 255 pixel if projected to the scene plane) of the camera was ca. 3.5 mm.

implies 31.25 cm for the vertical axis if aspect ratio is to be preserved.

Manual approach. Having pointed the steerable mirror to the desired location, manual keystone correction using the MDC-X software involves warping the image to be projected by manipulating the corners of the image until the desired effect is produced on the projection surface. In order to provide a template for manually carrying out keystone correction, we prepared a rectangular 50 cm \times 31.25 cm cutout of cardboard. For each target location, we placed this piece of cardboard in a manner that its axes were aligned with the principal axes of the scene (cf. the yellow and red lines in Figure 5(b)); we then manually warped the image for the given target location so that any corner of the augmentation deviated by at most 1 cm from the corresponding corner of the template. End-to-end, the process of setting the presets in the MDC-X software having carried out keystone correction manually took ca. 32 min for the 15 target locations.

Table 1: Deviations in measured lengths from 50 cm \times 31.25 cm across the 15 augmentations produced using our approach, provided in cm and in pixel units of the downwards-facing camera (pixel size 3.5 mm). Note that in no instance do mean and standard deviation exceed 1 pixel from the viewpoint of the camera.

	Top	Bottom	Left	Right
Mean _[cm]	0.03	0.07	0.09	0.06
Stdev _[cm]	0.33	0.17	0.17	0.17
Mean _[px]	0.1	0.19	0.26	0.18
Stdev _[px]	0.95	0.48	0.49	0.49

Table 2: Deviations in measured angles from 90° across the 15 augmentations produced using our approach.

	Top Left	Bottom Right
Mean _[deg]	-0.03	0.0
Stdev _[deg]	0.4	0.34

Our approach. We began by carrying out a calibration of the camera, acquiring
270 10 camera calibration images (cf. Section 2.1) of a chessboard calibration pattern with 6×4 corners (7×5 squares) and feeding the images as input to our camera calibration module. Separately, for each of the 15 target locations, we produced a projector calibration image (cf. again Section 2.1) by projecting a 11×4 asymmetrical circle pattern image to the location in question using
275 the steerable mirror, placing a chessboard pattern beside the projected pattern, and acquiring the image using the downwards-facing camera. We then fed these images alongside the output of the camera calibration module to our projector calibration module. For each of the target locations, the steerable mirror was made to point to that location, the asymmetrical circle pattern image was projected to the scene plane, an image was acquired using the camera, and
280 the location was registered in the MDC-X software as a preset. The output of the projector calibration module is a homography per input projector calibration image (cf. Section 2.2). Next, we warped the images to be projected to the respective locations using their corresponding homography, using a third
285 dedicated custom module. These warped images were finally imported into the MDC-X software and associated with their respective location presets (cf. Figure 5(b)).

Tables 1 and 2 give the deviations in measured lengths and angles, respectively, from the intended quantities. Lengths were measured using a measuring
290 tape for the top, bottom, left, and right sides of the augmentations; angles were measured using an angle gauge at the augmentations' top-left and bottom-right corners (the measuring tape and angle gauge are both visible in Figure 5(b)). Note that if deviations in measured lengths are expressed in units of pixels of the downwards-facing camera, mean and standard deviation in no instance exceed 1 pixel. The total amount of time expended for carrying out all the above
295 steps amounted to ca. 20 min, with ca. 2 min going to acquisition of the camera calibration images, and ca. 5 min going to that of projector calibration images. The remainder of the time was spent running our modules or working with the MDC-X software. Note that once the camera is calibrated, that calibration can

300 be reused if the camera’s intrinsics remain fixed, in particular if no change is
made to the zoom factor or focus settings of the camera.

4. Conclusion

We presented a spatial AR system for planar scenes that produces the effect of keystone correction analytically as a function of the geometry relating
305 projector and scene plane, exploiting a steerable mirror system to enable augmentation exceeding the bounds of the projector’s own immediate field of view. Our method produces this effect in a manner that enables intuitive placement of the augmentations in accordance with the X - and Y -axes of a camera placed to face downwards towards the scene plane. Moreover, our method allows for specifying the desired dimensions of augmentations in metric terms, thus enabling
310 consistent scaling. Our evaluation demonstrated our approach to produce compelling results—with mean and standard deviation of errors in measured lengths within the downwards-facing camera’s pixel size—at less time than a more cumbersome manual approach to keystone correction.

315 A natural extension of this work would be to consider the impact of varying calibration patterns, their dimensions, and their scale relative to the camera. Still another would be to address the augmentation of non-planar scenes. To handle non-planar scenes would call for a change in how scene geometry is recovered and how warping of the image to be projected is carried out; the methodology we proposed for projector calibration could, however, be left
320 unchanged.

5. Acknowledgments

This work was supported by the Austrian Research Promotion Agency (FFG) through its endowed professorship in Human Centered Cyber Physical Production and Assembly Systems at TU Wien (FFG-852789).
325

References

- [1] D. Van Krevelen, R. Poelman, A survey of augmented reality technologies, applications and limitations, *International Journal of Virtual Reality* 9 (2) (2010) 1–20.
- 330 [2] F. Zhou, H. B.-L. Duh, M. Billinghurst, Trends in augmented reality tracking, interaction and display: A review of ten years of ISMAR, in: 2008 7th IEEE/ACM International Symposium on Mixed and Augmented Reality, IEEE, 2008, pp. 193–202.
- 335 [3] S. Schlund, W. Mayrhofer, P. Rupprecht, Möglichkeiten der Gestaltung individualisierbarer Montagearbeitsplätze vor dem Hintergrund aktueller technologischer Entwicklungen, *Zeitschrift für Arbeitswissenschaft* 72 (4) (2018) 276–286.
- 340 [4] T. Masood, J. Egger, Augmented reality in support of industry 4.0—implementation challenges and success factors, *Robotics and Computer-Integrated Manufacturing* 58 (2019) 181–195.
- [5] M. Gattullo, G. W. Scurati, M. Fiorentino, A. E. Uva, F. Ferrise, M. Bordegoni, Towards augmented reality manuals for industry 4.0: A methodology, *Robotics and Computer-Integrated Manufacturing* 56 (2019) 276–286.
- 345 [6] A. E. Uva, M. Gattullo, V. M. Manghisi, D. Spagnulo, G. L. Cascella, M. Fiorentino, Evaluating the effectiveness of spatial augmented reality in smart manufacturing: a solution for manual working stations, *The International Journal of Advanced Manufacturing Technology* 94 (1) (2018) 509–521.
- 350 [7] P. Rupprecht, H. Kueffner-McCauley, S. Schlund, Information provision utilizing a dynamic projection system in industrial site assembly, *Procedia CIRP* 93 (2020) 1182–1187.
- [8] P. Rupprecht, H. Kueffner-McCauley, M. Trimmel, S. Schlund, Adaptive spatial augmented reality for industrial site assembly, *Procedia CIRP*.

- 355 [9] O. Bimber, R. Raskar, Spatial Augmented Reality: Merging Real and Virtual Worlds, AK Peters/CRC Press, 2019.
- [10] C. Pinhanez, The everywhere displays projector: A device to create ubiquitous graphical interfaces, in: International Conference on Ubiquitous Computing, Springer, 2001, pp. 315–331.
- 360 [11] R. Kjeldsen, C. Pinhanez, G. Pingali, J. Hartman, T. Levas, M. Podlaseck, Interacting with steerable projected displays, in: Proceedings of Fifth IEEE International Conference on Automatic Face Gesture Recognition, IEEE, 2002, pp. 402–407.
- 365 [12] C. Pinhanez, R. Kjeldsen, A. Levas, G. Pingali, M. Podlaseck, N. Sukaviriya, Applications of steerable projector-camera systems, in: Proceedings of the IEEE International Workshop on Projector-Camera Systems at ICCV 2003, 2003.
- [13] R. I. Hartley, A. Zisserman, Multiple View Geometry in Computer Vision, 2nd Edition, Cambridge University Press, ISBN: 0521540518, 2004.
- 370 [14] R. Sukthankar, R. G. Stockton, M. D. Mullin, Smarter presentations: Exploiting homography in camera-projector systems, in: Proceedings Eighth IEEE International Conference on Computer Vision (ICCV), Vol. 1, IEEE, 2001, pp. 247–253.
- 375 [15] R. Raskar, P. Beardsley, A self-correcting projector, in: Proceedings of the 2001 IEEE Computer Society Conference on Computer Vision and Pattern Recognition (CVPR), Vol. 2, IEEE, 2001, pp. II–II.
- [16] D. C. Brown, Close-range camera calibration, Photogrammetric Engineering 37 (8) (1971) 855–866.
- 380 [17] J. Weng, P. Cohen, M. Herniou, et al., Camera calibration with distortion models and accuracy evaluation, IEEE Transactions on Pattern Analysis and Machine Intelligence 14 (10) (1992) 965–980.

- [18] B. Triggs, P. F. McLauchlan, R. I. Hartley, A. W. Fitzgibbon, Bundle adjustment—a modern synthesis, in: International Workshop on Vision Algorithms, Springer, 1999, pp. 298–372.
- [19] Z. Zhang, A flexible new technique for camera calibration, IEEE Transactions on Pattern Analysis and Machine Intelligence 22 (11) (2000) 1330–1334.
- [20] D. Moreno, G. Taubin, Simple, accurate, and robust projector-camera calibration, in: 2012 Second International Conference on 3D Imaging, Modeling, Processing, Visualization & Transmission, IEEE, 2012, pp. 464–471.
- [21] X. Zhang, L. Zhu, Projector calibration from the camera image point of view, Optical Engineering 48 (11) (2009) 117208.
- [22] S. Zhang, P. S. Huang, Novel method for structured light system calibration, Optical Engineering 45 (8) (2006) 083601.
- [23] G. Bradski, The OpenCV library, Dr. Dobb’s Journal of Software Tools 25 (2000) 120–125.
- [24] T. Collins, A. Bartoli, Infinitesimal plane-based pose estimation, International Journal of Computer Vision 109 (3) (2014) 252–286.